

## Rate Effects on Layering of a Confined Linear Alkane

Lionel Bureau\*

*Institut des Nanosciences de Paris, UMR 7588 CNRS-Universités Paris 6 and 7, 140 rue de Lourmel, 75015 Paris, France*  
(Received 19 June 2007; published 29 November 2007)

We perform drainage experiments of a linear alkane fluid (*n*-hexadecane) down to molecular thicknesses, and we focus on the role played by the confinement rate. We show that molecular layering is strongly influenced by the velocity at which the confining walls are approached: under high enough shear rates, the confined medium behaves as a structureless liquid of enhanced viscosity for a film thickness below  $\sim 10$  nm. Our results also lead us to conclude that a rapidly confined film can be quenched in a metastable disordered state, which might be related with recent intriguing results on the shear properties of confined films produced at different rates [Zhu and Granick, *Phys. Rev. Lett.* **93**, 096101 (2004)].

DOI: [10.1103/PhysRevLett.99.225503](https://doi.org/10.1103/PhysRevLett.99.225503)

PACS numbers: 81.40.Pq, 68.35.Af, 83.50.-v

From nanofluidics [1,2] to friction and boundary lubrication [3], the issue of fluid flow in nanometer-thick films attracts a growing interest. It is known that when liquids are confined to molecular thicknesses, their properties deviate markedly from those of the bulk state [4,5]. If two solid surfaces are approached at distances of a few nanometers in a liquid, so-called structural forces are observed, which are associated with the ordering of molecules into layers parallel to the confining walls [4,6–10]. Understanding how such a structuration affects the shear response of confined liquids has been the scope of a large number of studies, both numerical [11–13] and experimental. The latter have addressed this issue using the surface force apparatus (SFA) [14–20] or atomic force microscopy [21,22].

Most of the works mentioned above focus on the lubrication or viscoelastic properties of equilibrated films, i.e., which have reached their equilibrium layered structure before shear begins. However, in the course of a recent debate on reassessment of SFA measurements [23–25], it has been suggested that the velocity at which a liquid is brought to molecular thickness may strongly influence its shear response [23,24]. In their work, Zhu and Granick [23,24] find that thin films formed by rapid confinement exhibit a much higher effective viscosity than those produced quasistatically. The authors attribute this effect to the fact that rapid confinement yields less structured films.

This raises two questions: (i) how does molecular layering depend on the confinement rate, and (ii) if a more disordered film is produced by rapid confinement, what is the stability of such a “mechanically quenched” state?

These questions have motivated us to revisit drainage experiments, as performed initially by Chan and Horn [14], and to study how the thinning of *n*-hexadecane confined between mica surfaces is affected by the velocity at which the surfaces are approached. We show here that layering is indeed most sensitive to the confinement velocity: at high enough shear rates, structuring is completely hindered. For thicknesses in the range 3–10 nm the drainage dynamics is akin to that of a liquid whose effective viscosity increases

with the level of confinement. Furthermore, our results lead us to conclude that a nonstructured film of hexadecane, obtained by quenching rapidly down to  $\sim 2$  nm, is metastable and relaxes towards the layered equilibrium configuration via a nucleation and growth process.

The experiments were performed using a recently developed surface force apparatus [26]. As in previous versions of the instrument [27–29], two atomically smooth mica sheets are mounted in a crossed-cylinder geometry (radius of curvature  $R \simeq 1$  cm), and the surfaces are immersed in the liquid under study. Our apparatus allows for independent measurements of the normal force  $F$  (by means of a capacitive load cell of stiffness  $31\,000\text{ N}\cdot\text{m}^{-1}$ ) and intersurface distance  $d$  (using multiple beam interferometry) at a rate on the order of 30 Hz. This enables us to obtain  $F(d)$  profiles during drainage of the fluid, while the mica surfaces are approached by driving the remote point of the loading spring at a prescribed velocity  $V$  in the range  $0.05\text{--}20\text{ nm}\cdot\text{s}^{-1}$ . The mica sheets were prepared according to the following protocol. Muscovite mica plates (JBG-Metafix, France) were cleaved down to a thickness of  $\sim 10\ \mu\text{m}$ , cut into  $1\text{ cm}^2$  samples by means of surgical scissors, and coated on one side with a 40 nm-thick thermally evaporated silver layer. The sheets were fixed, silver side down, onto cylindrical glass lenses, using a UV setting glue (NOA 81, Norland. UV curing was followed by thermal aging at  $50\text{ }^\circ\text{C}$  for 12 hours in order to suppress visco-elasticity of the glue layer). The mica sheets were placed on the lenses so that their crystallographic axis would be aligned. Prior to the experiments, each mica sample was recleaved using adhesive tape [30] and mounted in the apparatus so that the region of closest distance between the lenses would be free of steps. The surfaces were brought into contact under an argon atmosphere, and the total mica thickness was deduced from the position of the fringes of equal chromatic order (FECO) using the multilayer matrix method [26,31]. The surfaces were then separated and the thickness of each mica sheet determined using the same method. A drop of liquid ( $\sim 30\ \mu\text{L}$ ) was finally injected between the surfaces, a

beaker containing  $P_2O_5$  was placed inside the apparatus which was then sealed and left for thermal equilibration for about 12 hours before measurements began. The liquid used was the linear alkane *n*-hexadecane (Sigma-Aldrich, >99%). It was chosen because its behavior under confinement has already been studied both in quasistatic [8–10] and drainage [14] experiments using the SFA. The product was filtered through a  $0.2 \mu\text{m}$  membrane immediately before injection. All the experiments reported below have been performed at  $T = 24 \pm 0.02^\circ\text{C}$ .

We present results obtained in the following conditions. Starting from an initial distance of 20–30 nm, the remote point of the normal loading spring was driven at a given speed  $V$ , until a normal force on the order of  $500 \mu\text{N}$  was reached. A change in the radius of curvature of the mica sheets, due to deformation of the glue layer, was measurable for loads larger than  $100 \mu\text{N}$ , and  $F = 500 \mu\text{N}$  yields a normal pressure of about 500 kPa.

Figure 1 shows three  $F(d)$  profiles measured at  $V = 0.05, 1, 5,$  and  $10 \text{ nm} \cdot \text{s}^{-1}$ . Layering of hexadecane is clearly observed at  $V = 0.05 \text{ nm} \cdot \text{s}^{-1}$ : for distances  $d \leq 3 \text{ nm}$ , the film thickness decreases by steps of 4–5 Å as the force increases, in agreement with previous studies [6,10]. Such a steplike thinning of the fluid totally disappears for  $V \geq 1 \text{ nm} \cdot \text{s}^{-1}$  to yield a smooth monotonic repulsive profile (see Fig. 1). Besides, we note that for a given film thickness, the normal force is all the larger as the confining velocity is high.

So, for high enough approach velocities, layering is dynamically hindered, and the confined medium stays structureless.

Now, at large  $V$ , hydrodynamic forces may account for a non-negligible part of the measured repulsive forces. On Fig. 2, we compare the force-distance curve measured at  $V = 10 \text{ nm} \cdot \text{s}^{-1}$  with that corresponding to the squeeze

flow of hexadecane, using the bulk viscosity  $\eta = 3.5 \times 10^{-3} \text{ Pa} \cdot \text{s}$ . The hydrodynamic force, assuming no-slip boundary conditions, is given by [14]:

$$F_H = 6\pi R^2 \eta \frac{\dot{d}}{d}, \quad (1)$$

where  $R = 1 \text{ cm}$  is the radius of curvature of the cylindrical lenses, and  $\dot{d}$  is the actual approach velocity of the surfaces. Comparison of  $F_H(d)$  and  $F(d)$  is performed for  $F < 100 \mu\text{N}$ , which, as mentioned above, ensures that the radius  $R$  is not affected by deformation of the surfaces. Figure 2 shows that for  $d > 10 \text{ nm}$ , the repulsive force can be ascribed to hydrodynamic flow of the bulk liquid, whereas for  $d \leq 10 \text{ nm}$ , the measured forces are larger than  $F_H$ . A modification of Eq. (1), as suggested by Chan and Horn [14], to account for shifted no-slip boundary conditions—i.e., replacing  $d$  by  $d - 2d_s$ , where  $d_s$  is the thickness of an immobile layer near each wall—does not allow either to fit the experimental  $F(d)$  profiles at short distances.

This points to the existence of a thickness regime in which the nonstructured confined fluid does not exhibit bulklike flow properties. Tentatively, we use expression (1) to estimate an effective viscosity of confined hexadecane from the experimental  $F(d)$  data:  $\eta_{\text{eff}} = Fd/(6\pi R^2 \dot{d})$ . This is plotted in Fig. 3 as a function of thickness, for three driving velocities. It is seen that comparable profiles for  $\eta_{\text{eff}}(d)$  are obtained, independently of  $V$ , which gives support to our analysis in terms of an effective viscosity. Moreover, it appears that  $\eta_{\text{eff}}$  starts to deviate noticeably from the bulk value at short distances, and increases by more than 1 order of magnitude as  $d$  goes roughly from 10 to 3 nm.

This is in apparent contradiction with the results of Chan and Horn [14], who found that, assuming the existence of

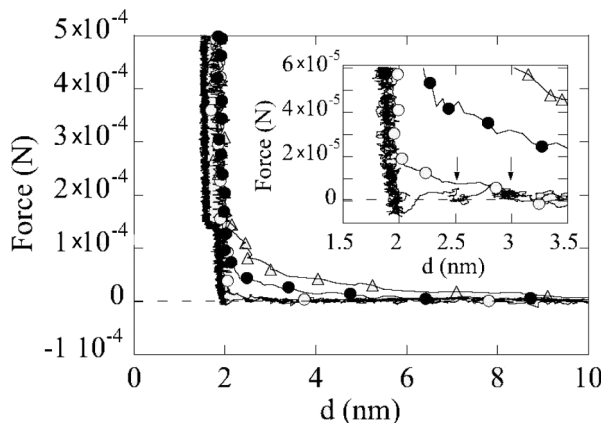


FIG. 1. Force vs distance curves measured during approach at  $V = 0.05 \text{ nm} \cdot \text{s}^{-1}$  (full line),  $V = 1 \text{ nm} \cdot \text{s}^{-1}$  (full line with  $\circ$  markers),  $V = 5 \text{ nm} \cdot \text{s}^{-1}$  (full line with  $\bullet$  markers), and  $V = 10 \text{ nm} \cdot \text{s}^{-1}$  (full line with  $\triangle$  markers). Inset: close-up view of the same data set. Arrows indicate the first layering transitions detected, between  $d \approx 3$  and  $2.5 \text{ nm}$ .

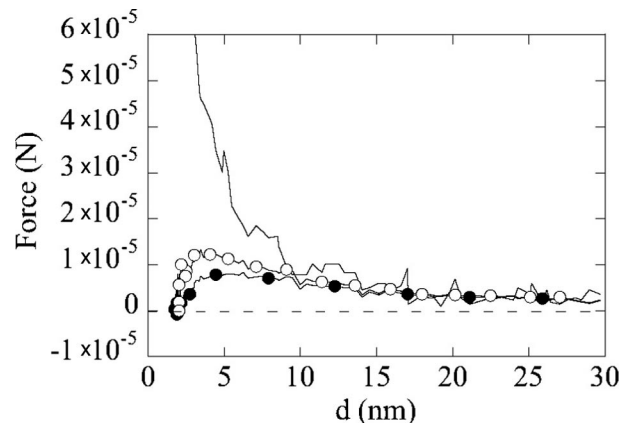


FIG. 2. Force vs distance curve measured during approach at  $V = 10 \text{ nm} \cdot \text{s}^{-1}$  (full line). Hydrodynamic force  $F_H$  calculated using expression (1) and a no-slip boundary condition (full line with  $\bullet$ ).  $F_H$  calculated using a no-slip plane shifted inside the gap by  $d_s = 0.8 \text{ nm}$  (full line with  $\circ$ ).

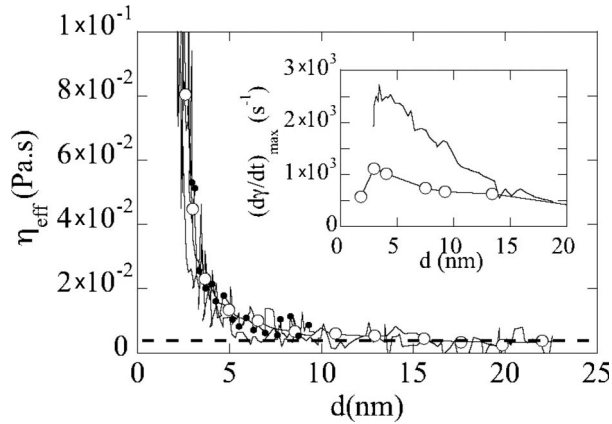


FIG. 3. Effective viscosity vs thickness for  $V = 2 \text{ nm} \cdot \text{s}^{-1}$  (line with  $\bullet$  markers),  $V = 5 \text{ nm} \cdot \text{s}^{-1}$  (full line), and  $V = 10 \text{ nm} \cdot \text{s}^{-1}$  (line with  $\circ$  markers). The dashed line indicates the bulk value  $\eta = 3.5 \times 10^{-3} \text{ Pa} \cdot \text{s}$ . Inset:  $\dot{\gamma}_{\max}$  vs distance for  $V = 10 \text{ nm} \cdot \text{s}^{-1}$  (full line) in our experiment, and that deduced from Fig. 9 of Ref. [14], for which  $V = 16 \text{ nm} \cdot \text{s}^{-1}$  (line with  $\circ$  markers).

two immobile layers on each wall, bulk viscosity could account for the fluid drainage down to thicknesses of 2–3 nm. However, it is important to note here that our apparatus has a stiffness which is more than 2 orders of magnitude larger than that used in Ref. [14]. From the force balance  $F_H = K(Vt - [d - d_{t=0}])$ , where the right-hand-side term is the restoring force of the cantilever spring of stiffness  $K$ , it follows that for a given distance  $d$  and driving velocity  $V$ , the lower  $K$ , the lower the approach velocity  $\dot{d}$ , as well as the maximum shear rate to which the fluid is submitted:  $\dot{\gamma}_{\max} \approx \sqrt{R/d\dot{d}}/d$  [32]. In the inset of Fig. 3, we have plotted  $\dot{\gamma}_{\max}(d)$  for  $V = 10 \text{ nm} \cdot \text{s}^{-1}$ . It appears that  $\eta_{\text{eff}}$  becomes larger than  $\eta_{\text{bulk}}$  when  $\dot{\gamma}_{\max} \geq 10^3 \text{ s}^{-1}$ . An analysis of the data of Chan and Horn in order to evaluate  $\dot{\gamma}_{\max}$  shows that, in their experiments,  $\dot{\gamma}_{\max} \leq 10^3 \text{ s}^{-1}$ , and that its maximum value is reached at distances  $d \sim 3 \text{ nm}$  (see inset of Fig. 3). Their study and ours are actually compatible, and the present work highlights the advantage of a high stiffness SFA, which gives access to a regime which could not be investigated in previous studies.

Furthermore, from the shear rate value of  $10^3 \text{ s}^{-1}$  at which  $\eta_{\text{eff}} > \eta_{\text{bulk}}$ , we estimate the relaxation time of hexadecane molecules to be  $1/\dot{\gamma}_{\max} \approx 10^{-3} \text{ s}$  when  $d < 10 \text{ nm}$ , i.e., many orders of magnitude larger than the Rouse time of bulk  $C_{16}$  chains [33]. This is in qualitative agreement with previous studies on relaxation in confined fluids [17].

Coming back to Fig. 1, it is clear that under a normal force of  $500 \mu\text{N}$ , the thickness of the film is  $1.65 \text{ nm}$  when  $V = 0.05 \text{ nm} \cdot \text{s}^{-1}$  and  $1.9 \text{ nm}$  when  $V = 10 \text{ nm} \cdot \text{s}^{-1}$ . In order to determine whether the thicker, rapidly quenched film evolves with time, we have performed the following experiment: at  $V = 10 \text{ nm} \cdot \text{s}^{-1}$ , hexadecane was confined

until a normal force of  $500 \mu\text{N}$  was reached. The load was then maintained at this value by means of a feedback control loop, and we monitored the time evolution of the film thickness  $d(t)$ , which is plotted on Fig. 4. The  $d(t)$  curve exhibits three important features: (i) once the force set point has been reached ( $t = 0$  on Fig. 4), the film thickness stays constant at  $1.9 \text{ nm}$  for  $\sim 20 \text{ s}$ ; (ii) for  $t \geq 20 \text{ s}$ ,  $d$  decreases linearly with time ( $\dot{d} = 3 \text{ pm} \cdot \text{s}^{-1}$ ), until it reaches a constant value of  $1.65 \text{ nm}$ ; (iii) the final value of  $d$  corresponds to the thickness of 4 molecular layers obtained under quasistatic loading.

Such a behavior suggests the following tentative picture. The abrupt stop of the thickness decrease, together with its quasilinear shape, leads us to rule out relaxation via diffusivelike evacuation of free volume towards the contact edges, which would yield a gradual self-deceleration. On the contrary, such a behavior appears consistent with a nucleation and growth process by which the rapidly confined film performs a transition from a higher volume, metastable disordered state, to a lower volume stable layered structure. A similar mechanism has already been evidenced in the layer-by-layer collapse of confined liquids [20]. In this context, one is tempted to identify the initial  $20 \text{ s}$  “incubation” time with a nucleation delay. However, since our signal is an average over a  $(5 \mu\text{m})^2$  zone close to the contact center, we cannot exclude that it might correspond to the time required for the growing layered patch to reach a large enough radius (comparable to the mica thickness  $\sim 3 \mu\text{m}$ ) for the local bending of the mica sheets to be detectable.

In order to check further the validity of the above picture, we have performed the following experiment: hexadecane was confined at a much lower rate, namely  $V = 1 \text{ nm} \cdot \text{s}^{-1}$ , and  $d(t)$  monitored under  $F = 500 \mu\text{N}$ . It

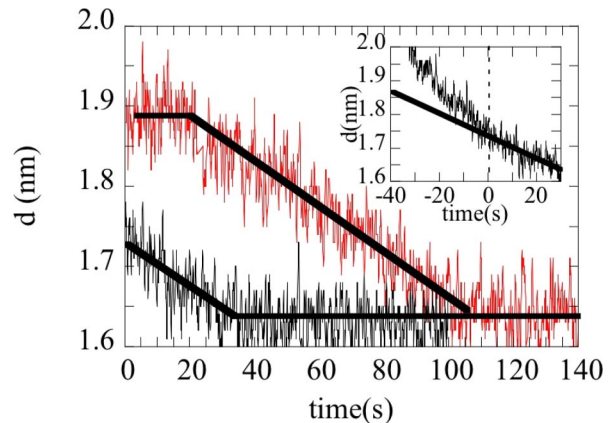


FIG. 4 (color online). Thickness vs time for two films confined at  $V = 10 \text{ nm} \cdot \text{s}^{-1}$  (upper curve, red line) and  $V = 1 \text{ nm} \cdot \text{s}^{-1}$  (lower curve, black line). Loading is stopped and  $F = 500 \mu\text{N}$  is maintained at  $t \geq 0$ . Inset: data for  $V = 1 \text{ nm} \cdot \text{s}^{-1}$  showing that for  $t < 0$ , during loading, the thickness decrease is faster than that observed under the final constant force. Thick lines are guides for the eye.

is seen on Fig. 4 that, once the force set point is reached, the film thickness decreases from  $d = 1.75$  nm at the same velocity and until the same final value as those observed in the higher rate experiment. This provides support to the nucleation and growth scenario: it is consistent with the growth of a stable phase which, under a given applied pressure, occurs at a velocity which is independent of the rate at which the film has been produced. Moreover, we note on Fig. 4 that no “nucleation phase” is observed for  $V = 1$  nm  $\cdot$  s $^{-1}$ , and that  $d$  decreases with time during the loading phase, at a velocity which is about twice that observed under constant load. This suggests that nucleation of the stable phase has occurred before reaching the load set point, and that propagation, helped by the slowly increasing pressure, takes place at a larger velocity during loading.

In conclusion, we have performed drainage experiments which unambiguously show that layering of a confined liquid is hindered when the medium is submitted to high enough shear rates. Taking advantage of a newly developed surface force apparatus, we evidence that the effective viscosity of hexadecane may deviate from its bulk value at thicknesses on the order of 10 nm in situations of fast out-of-equilibrium confinement. Moreover, our results indicate that a disordered film formed by a rapid mechanical quench is in a metastable state. Whether the formation of such metastable states is at the origin of the results of Zhu and Granick [23,24] mentioned in the introduction is still to be clarified. This calls for further experiments investigating how the yield stress buildup and the steady state shear response of molecularly thin films are affected by the confinement rate.

The author wishes to thank C. Caroli and T. Baumberger for fruitful discussions, and B. Calmettes for his contribution to the experimental work.

---

\*bureau@insp.jussieu.fr

- [1] J. C. T. Eijkel and A. van den Berg, *Microfluid. Nanofluid.* **1**, 249 (2005), and references therein.
- [2] M. Majumder, N. Chopra, R. Andrews, and B. J. Hinds, *Nature (London)* **438**, 44 (2005).
- [3] B. N. J. Persson, *Sliding Friction*, Nanoscience and Technology Series (Springer, New York, 2000).
- [4] J. N. Israelachvili, *Intermolecular and Surface Forces* (Academic, New York, 1992).
- [5] M. Alcoutlabi and G. B. McKenna, *J. Phys. Condens. Matter* **17**, R461 (2005).
- [6] J. P. Gao, W. D. Luedtke, and U. Landman, *J. Chem. Phys.* **106**, 4309 (1997), and references therein.
- [7] F. Porcheron, B. Rousseau, and A. H. Fuchs, *Mol. Phys.* **100**, 2109 (2002), and references therein.
- [8] R. G. Horn and J. N. Israelachvili, *Chem. Phys. Lett.* **71**, 192 (1980).
- [9] R. G. Horn and J. N. Israelachvili, *J. Chem. Phys.* **75**, 1400 (1981).
- [10] H. K. Christenson, D. W. R. Gruen, R. G. Horn, and J. N. Israelachvili, *J. Chem. Phys.* **87**, 1834 (1987).
- [11] P. A. Thompson, M. O. Robbins, and G. S. Grest, *Isr. J. Chem.* **35**, 93 (1995).
- [12] S. T. Cui, C. McCabe, P. T. Cummings, and H. D. Cochran, *J. Chem. Phys.* **118**, 8941 (2003).
- [13] A. Jabbarzadeh, P. Harrowell, and R. I. Tanner, *Phys. Rev. Lett.* **94**, 126103 (2005).
- [14] D. Y. C. Chan and R. G. Horn, *J. Chem. Phys.* **83**, 5311 (1985).
- [15] C. Cottin-Bizonne, S. Jurine, J. Baudry, J. Crassous, F. Restagno, and E. Charlaix, *Eur. Phys. J. E* **9**, 47 (2002).
- [16] R. G. Horn and J. N. Israelachvili, *Macromolecules* **21**, 2836 (1988).
- [17] A. L. Demirel and S. Granick, *Phys. Rev. Lett.* **77**, 2261 (1996).
- [18] G. Reiter, A. L. Demirel, and S. Granick, *Science* **263**, 1741 (1994).
- [19] J. Klein and E. Kumacheva, *J. Chem. Phys.* **108**, 6996 (1998).
- [20] T. Becker and F. Mugele, *Phys. Rev. Lett.* **91**, 166104 (2003).
- [21] A. Maali, T. Cohen-Bouhacina, G. Couturier, and J. P. Aime, *Phys. Rev. Lett.* **96**, 086105 (2006).
- [22] R. Lim, S. F. Y. Li, and S. J. O’Shea, *Langmuir* **18**, 6116 (2002).
- [23] Y. Zhu and S. Granick, *Phys. Rev. Lett.* **93**, 096101 (2004).
- [24] Y. Zhu and S. Granick, *Langmuir* **19**, 8148 (2003).
- [25] J. Israelachvili, N. Maeda, and M. Akbulut, *Langmuir* **22**, 2397 (2006); S. Granick, Y. Zhu, Z. Lin, S. C. Bae, J. Wong, and J. Turner, *Langmuir* **22**, 2399 (2006); D. Gourdon and J. Israelachvili, *Phys. Rev. Lett.* **96**, 099601 (2006); J. Wong, S. C. Bae, S. Anthony, Y. Zhu, and S. Granick, *Phys. Rev. Lett.* **96**, 099602 (2006).
- [26] L. Bureau, *Rev. Sci. Instrum.* **78**, 065110 (2007).
- [27] D. Tabor and R. H. S. Winterton, *Proc. R. Soc. A* **312**, 435 (1969).
- [28] J. N. Israelachvili and D. Tabor, *Proc. R. Soc. A* **331**, 19 (1972).
- [29] J. N. Israelachvili and G. E. Adams, *J. Chem. Soc., Faraday Trans. 1* **74**, 975 (1978).
- [30] P. Frantz and M. Salmeron, *Tribol. Lett.* **5**, 151 (1998).
- [31] M. Heuberger, *Rev. Sci. Instrum.* **72**, 1700 (2001).
- [32]  $\dot{\gamma}$  reaches its maximum value at a lateral distance  $r \approx \sqrt{Rd}$  of a few microns away from the point of closest approach [14].
- [33] C. Baig, B. Jiang, B. J. Edwards, D. J. Keffer, and H. D. Cochran, *J. Rheol. (N.Y.)* **50**, 625 (2006).